Medical Engineering & Physics 31 (2009) 1140–1147

Contents lists available at ScienceDirect

Medical Engineering & Physics

journal homepage: www.elsevier.com/locate/medengphy

Assessment of cortical bone elasticity and strength: Mechanical testing and ultrasound provide complementary data

Quentin Grimal[a,b,*], Sylvain Haupert[a,b], David Mitton[c], Laurent Vastel[d], Pascal Laugier[a,b]

[a] UPMC Univ Paris 06, UMR 7623, LIP, F-75005, Paris, France
[b] CNRS, UMR 7623, Laboratoire d'Imagerie Paramétrique, F-75005, Paris, France
[c] Arts et Metiers ParisTech, CNRS, LBM, 151 Bd de l'Hopital 75013 Paris, France
[d] Banque de tissus osseux Cochin AP-HP, Hôpital Cochin, 27 rue du Faubourg St Jacques, 75014 Paris, France

ARTICLE INFO

Article history:
Received 22 April 2008
Received in revised form 12 May 2009
Accepted 11 July 2009

Keywords:
Cortical bone
Ultrasound
Elasticity
Strength

ABSTRACT

Cortical bone is a compact tissue with anisotropic macroscopic mechanical properties determined by a microstructure and the quality of a mineralised collagen matrix. Anisotropic elastic properties and strength are usually measured on different groups of sample which can hardly be pooled; as a consequence little is known on the relationships between strength and elasticity in the different anatomical directions. A method is presented to measure on a same cortical bone sample: (1) Young's modulus and strength (σ_{max}) in the longitudinal direction; (2) stiffness (C_{11}) in the transverse direction. Longitudinal and transverse direction are taken along and perpendicular to the diaphysis axis, respectively. Ultrasonic techniques yield Young's modulus (E_a) and C_{11}; three-point bending tests yield Young's modulus (E) and σ_{max}. The relationships between strength, elasticity and density and their anatomical distributions were investigated for 36 human femur samples. (i) A marginal negative correlation was obtained for E_a and C_{11} ($R=-0.21$; $p=0.08$); (ii) σ_{max} was significantly correlated to E and E_a ($R\sim0.5$; $p<0.005$) but not to C_{11} ($p>0.2$); (iii) density was not correlated with E and moderately with strength ($R=0.38$; $p<0.3$). Small density variability ($\pm30\,kg\,m^{-3}$) may partly explain the results. The techniques presented are suited to a systematic characterization of bone samples.

1. Introduction

Density is often considered to be an important determinant of bone mechanical properties. Empirical relationships have been proposed to derive cortical bone elasticity and strength based solely on density [1] or, alternatively, mineral density [2,3] obtained from X-ray computed tomography (CT). These relationships are commonly used to model bone properties in biomechanics finite element (FE) models [4–6]. In up to date FE models at the organ level, bone tissue is isotropic, the Poisson's ratio is assumed constant, and strength and Young's modulus are derived from CT-numbers. Model prediction inaccuracies due to neglecting anisotropy are hard to evaluate. Nevertheless Kober et al. [7] demonstrated that anisotropy should be accounted for so as to predict a realistic behaviour of the mandible. The correlation between strength in the longitudinal direction of bone (along the diaphysis axis) and elasticity in the same direction is usually good [8,9], hence it may appear reasonable to derive both values from density data only. In contrast poor and non-significant correlations between elastic coefficients in the longitudinal and transverse (perpendicular to the diaphysis axis) directions have been reported [10,11]. These results point out the possible limitations of the hypothesis of isotropy for cortical bone tissue, which is used in particular in FE models. However, because it is technically difficult to assess bone properties, there is little data to verify the hypothesis.

The anisotropic elasticity of bone cubes has been fully characterized with ultrasound [12,13]. However the strength is usually measured with traction or three-point bending from long and thin samples [14]. As a consequence anisotropic elasticity and strength are usually assessed on different volumes of material. Unfortunately data from different investigations can hardly be pooled due to the important variability of bone properties.

The purpose of this work is to investigate the relationships between elastic properties in two orthogonal directions (i.e., Young's modulus in the longitudinal direction and stiffness C_{11} in the transverse direction), strength, and density in femur cortical bone assessed on the same group of samples. Assessment of elastic properties in two orthogonal directions as well as strength in one direction for each sample was possible thanks to a combination of mechanical and ultrasonic measurements (US). An ancillary objective of the work was the comparison between ultrasonic

* Corresponding author at: Université Pierre et Marie Curie-Paris6, LIP UMR7623, Paris F-75005, France. Tel.: +33 144414972; fax: +33 146335673.
E-mail address: quentin.grimal@upmc.fr (Q. Grimal).

1350-4533/$ – see front matter © 2009 IPEM. Published by Elsevier Ltd. All rights reserved.
doi:10.1016/j.medengphy.2009.07.011

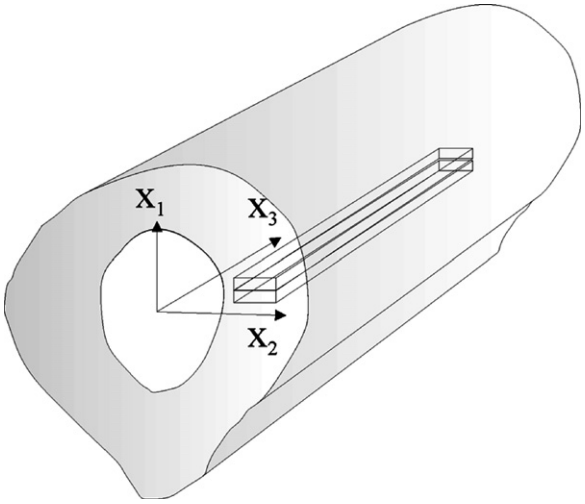

Fig. 1. Schematic representation of 2 plate-like samples (approximate dimensions 50 mm × 5 mm × 2 mm) cut along the diaphysis.

and mechanical assessment of elasticity. The data presented in the paper illustrates the ability of coupled ultrasound–mechanical measurements to contribute to a better documentation of bone mechanical properties. Others, providing a minimum competency in ultrasound and mechanical testing, can set such measurements in practice.

2. Methods

2.1. Sample preparation

Samples were obtained from four femurs removed during multi-organ collection, which complied with the requirements of the French Transplant Administration. Femurs were from three donors: two women (23 years, femur I; 28 years, femur II), and one man (63 years, femurs III and IV). Four cylindrical parts of 5 cm each, labelled from P1 (proximal) to P4 (distal) were cut in the mid-diaphysis of each femur. Eighty-eight plate-like samples, with dimensions approximately 50 mm × 5 mm × 2 mm were cut from the anterior (A), lateral (L), posterior (P), and medial (M) sectors of parts P1–4 as pairs of adjacent pieces. See Fig. 1 for sample orientation and definition of the reference frame.

Cuts were done under continuous irrigation with a linear saw (ISOMET 4000, Buehler SARL, Dardilly, FRANCE). Prior to the preparation and in between tests, samples were kept frozen at −20 °C. Sample dimensions and mass were measured with a digital calliper (precision 0.01 mm) and a balance (AG245, Coubart SARL, France, precision 5×10^{-5} g), respectively. Apparent density ρ was calculated as the ratio of mass to volume.

Forty-four pairs of adjacent samples were split evenly in groups A and B. Group A was subjected to US and mechanical measurements but Group B could only be subjected to US measurements because it was required for another study. Results are presented for Group Ac = Group A + Group B (ultrasound data) and Group AcMech = Group A (ultrasound and mechanical measurements).

2.2. Ultrasonic measurements in the longitudinal direction

Fresh samples were brought to room temperature and placed between two 60 kHz ultrasound plane transducers (17 mm diameter, Physical Acoustic Group, R6, USA) as shown in Fig. 2(a), and roughly at the centre of the transducers' surfaces. An echographic gel (Drexco Medical, Crosne, France) ensured acoustic coupling. One piezoelectric element was excited with a pulser (Panametrics 5052 PR, Waltham, MA, USA) and the other one was connected to an oscilloscope (Tektronix TDS 1012, Beaverton, OR, USA, sampling rate 1 GHz). The time at which the electrical pulse was initiated served as a reference to calculate time of flights (TOF). An iterative method was developed to retrieve the onset of the signal transmitted through the specimen. First, the earliest time ξ_1 at which the signal crossed a fixed threshold (five standard deviations of noise) was determined. Then, for each iteration, the intersection ξ_{n+1} between a linear fit of the 3 μs-portion of signal before ξ_n and a linear fit of a 1 μs-portion of signal after ξ_n was determined. The procedure was found to converge for $n < 10$ for all signals; finally the TOF was defined to be ξ_{10}, see Fig. 2(b). Finally, the velocity V_l in the longitudinal direction ($\mathbf{x}_3$) of the sample was calculated as the ratio of sample length to TOF. The validity of this signal processing method was assessed by measuring two Perspex® samples differing only by their length. The velocity obtained as the ratio between the differences in length and TOF, which is free of any bias arising from the determination of the signal initiation or arrival times, differed by less than 1% from the velocities retrieved from a single measurement. The latter difference being less than the intrinsic precision of the method (see below) it was concluded that the signal processing was appropriate to retrieve the wave TOF.

The apparent elastic modulus was defined as $E_a = \rho \times V_l^2$, where the subscript 'a' ("acoustics") is used to distinguish this modulus from the Young's modulus measured with the mechanical method (Section 2.4). In the limiting case where the wavelength

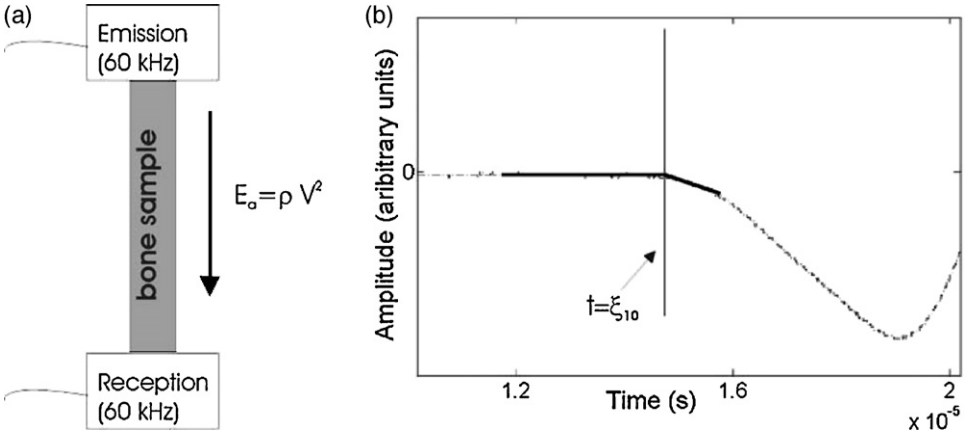

Fig. 2. (a) Schematic representation of the 60 kHz ultrasonic measurement; (b) signal at the transducer receiver; the vertical line indicates the arrival time determined by the signal processing method. Acoustical Young's modulus is obtained as $E_a = \rho \times V_l^2$, where V_l is the velocity of propagation between the two transducers.

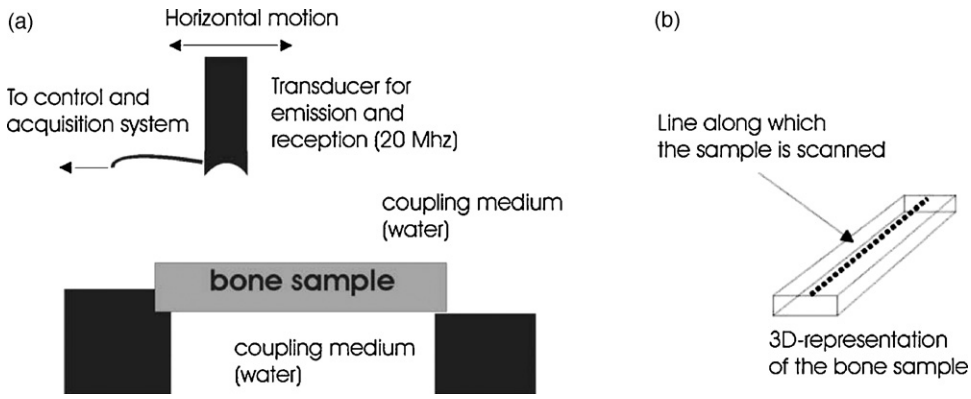

Fig. 3. (a) Schematic representation of the echo-mode setup (20 MHz). The bulk wave velocity V_t measured in double transmission is used to derive the stiffness coefficient C_{11} according to $C_{11} = \rho \times V_t^2$. (b) 3D representation of the sample and the dots showing the line along which the sample is scanned (90 measurement points).

is much larger (several orders of magnitude) than the characteristic dimension of the sample's cross-section, the wave is expected to propagate according to the bar mode [15] and the apparent modulus in that case is identical to the actual Young's modulus.

2.3. Through thickness ultrasound measurements

Samples were brought to room temperature and placed in a tank filled with water as shown in Fig. 3. A 20 MHz focused transducer (Panametrics, Waltham, MA, USA; focal length: 20 mm; −6 dB beam diameter at focus: 460 μm) operating in the transmit receiver mode was placed in a mechanical support connected to micrometric stepping motors allowing translations in 3D. Samples were oriented perpendicularly to the US beam axis ($\mathbf{x}_1$) using a mechanical tilt stage. The beam centre was placed approximately at half the sample width. A pulser-receiver (Panametrics 5900 PR, Waltham, MA, USA) delivered the excitation voltage. Echoes reflected by the sample were amplified by the receiver electronics and digitized at a sampling frequency of 1 GHz by a PCI card (Acquiris DP240, Geneva, Switzerland). Radio frequency (RF, Fig. 4) signals were recorded at 90 points uniformly distributed along the length (Fig. 3(b)). The first echo observed at about 15 μs corresponds to the reflection on the top bone surface. The echo signal due to the reflection on the bottom surface is highly attenuated and interferes with signals scattered by heterogeneities in the thickness. However, summing the 90 RF signals acquired along a scan line averages out the scattering noise and allows the detection of the bottom echo (see Fig. 5). Since the ultrasound beam diameter and wavelength are much smaller than the sample dimensions bulk wave propagation is observed here, as opposed to the bar wave propagation described in the previous section. The echoes' TOF were determined as the time points corresponding to the maxima of the cross-correlation of the signal with a reference signal. The average bulk wave velocity V_t in direction $\mathbf{x}_1$ was then obtained as the ratio of the average thickness to the difference in TOF. The average stiffness coefficient C_{11} of the sample in the transverse direction is then obtained according to $C_{11} = \rho \times V_t^2$ [15].

2.4. Mechanical test

Samples of Group A were subjected to three-point bending tests on a mechanical testing machine (INSTRON 5500-R, Instron Corp.,

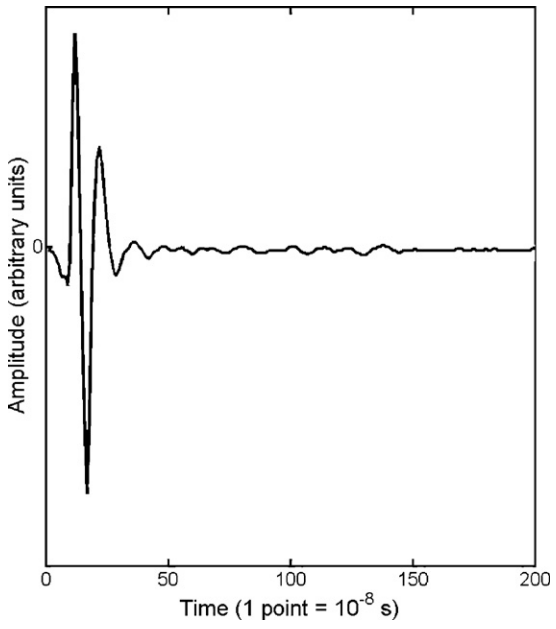

Fig. 4. One typical radio frequency (RF) signal in echo-mode through the sample's thickness (20 MHz). The large pulse corresponds to the first echo on the bone surface and the oscillations that follow are due to scattering.

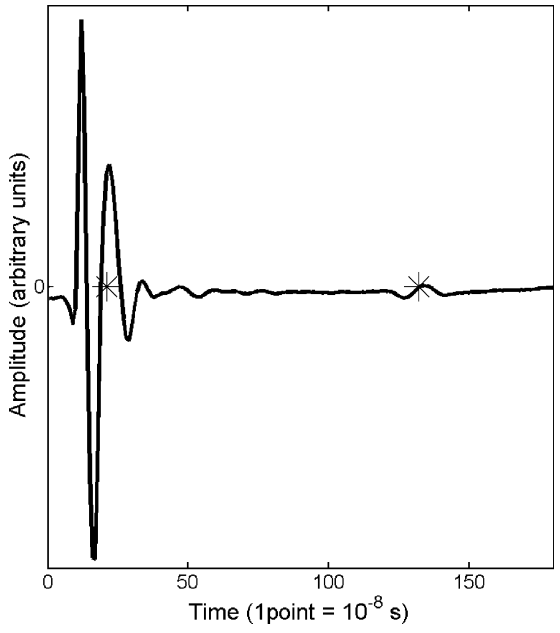

Fig. 5. After averaging the individual RF signals acquired along the scan line, the echoes from the two bone surfaces are clearly identified. The signs '*' indicate the TOF as given by the cross-correlation method.

Norwood, MA, USA). They were brought to room temperature and hydrated in a physiological solution at least 1 h before the measurements. Samples were placed on the testing machine for bending in the ($\mathbf{x}_1$,$\mathbf{x}_3$)-plane. Before mechanical testing, a 1-Newton loading was applied to ensure appropriate contact. Force and displacement were recorded until failure (speed: 6 mm/min). The span to thickness ratio of the samples (25:1) ensured a good estimation of the Young's modulus E and the breaking stress σ_{max} in direction $\mathbf{x}_3$ based on beam theory [14].

2.5. Validation of the measurement methods

Three Perspex® (3 mm × 5 mm × 50 mm) and three aluminium (2 mm × 5 mm × 50 mm) samples were used for the validation of the technique. Their elasticity was assessed with the three methods and compared to tabulated values. The reproducibility of the ultrasound set-ups were assessed using one Perspex® sample which was taken out of the set-up, repositioned and measured 20 times.

2.6. Statistics

Data were analysed using the statistical software NCSS 2000 (NCSS, Kaysville, UT, USA). The normality hypothesis could not be rejected for the distribution of any variable when the data on all the samples were pooled. Two-sample T-tests was used to determine whether Groups A and B were equivalent. Femur effect (between-sample variability) and anatomical effects (within-sample variability in the longitudinal and circumferential directions) on measured parameters were determined by one-way and two-way analysis of variance (ANOVA) followed by post hoc multiple comparison Tukey–Kramer tests. Correlation coefficients and corresponding confidence intervals where calculated with Matlab® Statistics Toolbox (The Mathworks Inc., Natick, MA, USA). The level of significance was taken at $p < 0.05$, unless otherwise stated.

3. Results

3.1. Validation of the measurement methods

The average Young's moduli measured with three-point bending were $E = 3.45$ GPa and $E = 72$ GPa for Perspex® and aluminium samples, respectively, which falls within the range of tabulated values 1.6–3.4 GPa and 69–79 GPa [16]. The accuracy was estimated to 3.6% for E and 1.8% σ_{max} based on the accuracy of the load and displacement cells.

The average acoustic Young's moduli measured with 60 kHz ultrasound were $E_a = 7$ GPa and $E_a = 87$ GPa for Perspex® and aluminium, respectively, which values are above the actual mechanical moduli. This result is consistent with the observations of Ashman et al. [13] and indicates that the cross-sectional dimensions of the samples are not small enough compared to the wavelength and accordingly a pure bar mode could not be observed. Hence for cortical bone it is expected that E_a be slightly larger than the actual (mechanical) Young's modulus because the wavelength in bone at 60 kHz is about 60 mm, compared to 45 mm and 110 mm in Perspex® and aluminium, respectively. The uncertainty was about 3% for V_l. Given an estimated uncertainty of 0.36% on the density, the resulting precision for E_a was about 6.2%.

The bulk wave velocities measured with the 20 MHz ultrasound set-up were 2737 ms^{-1} and 6677 ms^{-1} in average for Perspex® and aluminium samples, respectively. This values compare well with typical tabulated values of 2730 ms^{-1} [17] and 6420 ms^{-1} [18]. The estimated reproducibility for C_{11} was 0.86%, which was essentially due to the uncertainties in thickness measurements. It was concluded that the method assessed with precision the stiffness in the probing direction.

3.2. Presentation of measurement results

Sixty-eight samples (36 in Group A; 32 in Group B) were included in the analysis after 19 were eliminated due to sample misalignment

Table 1
Mean values (standard deviation) of measured quantities.

	V_l (m s^{-1})	V_t (m s^{-1})	E_a (GPa)	C_{11} (GPa)	ρ (kg m^{-3})	E (GPa)	σ_{max} (MPa)
Acoustic Group (Ac) 68 samples	3378 (82)	3570 (86)	22.1 (1,1)	24.7 (1.3)	1937 (30)		
Acoustic and Mechanics Group (AcMech) 36 samples	3372 (67)	3568 (86)	22.1 (0.9)	24.7 (1.3)	1939 (30)	17.3 (1.3)	195.3 (20.3)

Table 2
Correlation coefficients between measured quantities. The number of samples (n) in each group is indicated. Confidence intervals (95%) are estimated with the bootstrap technique with $n = 10{,}000$ bootstrap data samples.

	E_a	C_{11}	E	σ_{max}
E_a				
p				
n				
C_{11}	−0.21* (−0.40 −0.02)			
p	0.0812			
n	68			
E	0.63*** (0.37 0.79)	−0.14		
p	3×10^{-5}	0.39		
n	36	36		
σ_{max}	0.49*** (0.20 0.70)	0.20	0.53*** (0.20 0.75)	
p	0.0023	0.2416	9×10^{-4}	
n	36	36	36	
ρ			0.26	0.38** (0.01 0.70)
p			0.13	0.0221
n			36	36

* $p < 0.1$.
** $p < 0.05$.
*** $p < 0.01$.

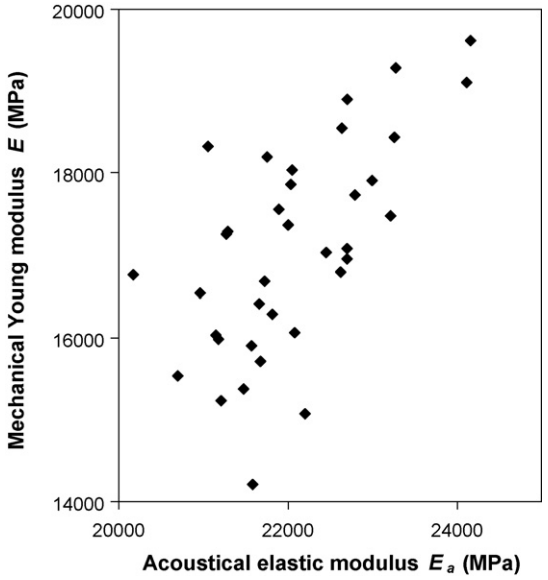

Fig. 6. Mechanical Young's modulus (E) vs. US modulus (E_a).

or presence of air bubbles in the wave path, and 1 due to a mistake in measuring density. Samples in Groups A and B were not significantly different regarding density and US measurements. Mean values and standard deviation of measured quantities are reported in Table 1.

This paragraph presents the correlations between the different quantities measured. Pearson correlation coefficients (R) are reported in Table 2. Presentation of the correlations for elastic coefficients was preferred over velocities for the sake of clarity, although the two elastic coefficients are calculated from velocities using the same density value for each sample. Mechanically measured (E) vs. acoustically measured (E_a) Young's moduli are given in Fig. 6. They were significantly correlated ($R = 0.63$, $p < 10^{-4}$). Acoustically measured elasticity in the longitudinal (E_a) and transverse (C_{11}) directions showed a negative and marginal ($R = -0.21$; $p = 0.0812$) correlation, and C_{11} was not correlated with the mechanical modulus E ($p > 0.3$). Strength in the longitudinal direction (σ_{max}) vs. elasticity in the same direction (E_a and E) is shown in Fig. 7; σ_{max} was significantly correlated to E_a ($R = 0.49$; $p < 0.003$) and to

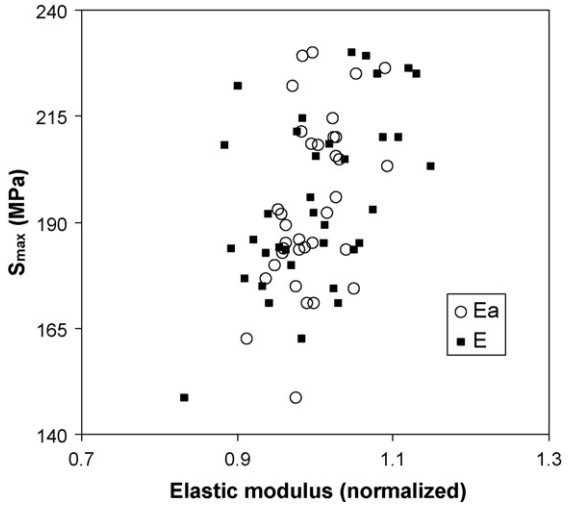

Fig. 7. Longitudinal elastic moduli (E_a and E) vs. maximal stress (σ_{max}). Moduli E_a and E are reported on the x-axis as quantities normalized with respect to the mean value of each data set: $E_a/\langle E_a \rangle$ and $E/\langle E_a \rangle$, where $\langle \bullet \rangle$ denotes the mean value of a set.

E ($R = 0.53$; $p < 10^{-3}$). However elasticity in the transverse direction (C_{11}) was not correlated to strength in the longitudinal direction (σ_{max}). Density was significantly correlated with σ_{max} ($R = 0.38$; $p < 0.03$) but not to E ($p > 0.1$).

The four groups of samples from parts P1–4 of the diaphysis contained 5, 14, 14 and 3 samples, respectively, for AcMech and 8, 27, 25, and 8 samples, respectively, for Ac. Only E_a had significant variations along the diaphysis ($F = 5.11$, $p = 0.0031$): the mean value of E_a for P2 (21.5 ± 1.0 GPa) was smaller than for parts P3 (22.4 ± 0.9 GPa) and P4 (22.6 ± 0.7 GPa). Other quantities did not vary along the femur length. Box plots of the five measured quantities grouped per anatomical quadrants, anterior (A), medial (M), lateral (L), and posterior (P) are shown in Fig. 8. The groups for A, M, L, and P contained 6, 11, 12, and 7 samples, respectively, for AcMech and 11, 21, 21 and 15 samples, respectively, for Ac. Significant variations were found around the circumference for C_{11} ($F = 7.93$, $p = 10^{-4}$), E_a ($F = 5.62$, $p = 1.7 \times 10^{-3}$) and E ($F = 4.14$, $p = 0.014$). Values of C_{11} for M were significantly higher than for A and L. Values of E_a for A were significantly higher than for P and M. Values of E for A were significantly higher than for L and M. Other measured quantities did not vary significantly with the anatomical quadrant. Fig. 9 gives a graphical representation of the distribution of the properties.

The femurs were significantly different regarding ρ and σ_{max} ($F = 5.84$, $p = 0.0014$; $F = 3.42$, $p = 0.028$, respectively): the mean density of femur III (1922 ± 32 kg m^{-3}) was significantly less than that of femurs II and IV (1953 ± 19 and 1958 ± 15 kg m^{-3}, respectively). The mean maximum stress for femur II was significantly above that of femur IV (209 ± 16 and 185 ± 20 MPa, respectively).

4. Discussion

The Young's modulus E measured with three-point bending was systematically lower than its ultrasonic counterpart E_a. The higher values of E_a are in part due to the fact that the wavelength is not large enough compared to sample's transverse dimension. A number of factors such as temperature and viscoelasticity may also have affected the values. Nevertheless both the values of E_a and E are consistent with values usually reported in the literature: the mean value $E = 17.3$ GPa compares well with $E = 16.6$ GPa and $E = 18.6$ GPa determined with mechanical methods by Dong and Guo [11] and Cuppone et al. [19], respectively. The modulus $E_a = 22.1$ GPa compares favourably with moduli measured with ultrasound by others: $E_a = 20$ GPa [13] (2.25 MHz), $E_a = 22.2$ GPa [20] (2.25 MHz) and $E_a = 19.9$ GPa [21] (50 kHz), where the central frequency of the transducer is given between parenthesis. The mean value $C_{11} = 24.6$ GPa (20 MHz) in the present study compares favourably to $C_{11} = 24.7$ GPa [20] (2.25 MHz) and $C_{11} = 23.4$ GPa [22] (5 MHz). This suggests that the high frequency used in this project (20 MHz) does not have a major effect on the measured bulk wave velocity in the range of frequencies considered (1–20 MHz).

The correlation coefficient found between E and E_a ($R = 0.63$) is higher than that reported by Ashman et al. [13] ($R = 0.53$) based on samples with moduli which had a slightly higher variability (14–23 GPa) compared to the present study (14–20 GPa). (The later reference is, as far as we know, the only work that confronts ultrasonic and mechanical measurement of the elasticity of cortical bone.) The outcome of a stochastic simulation reported in the appendix revealed that the lack of correlation between E and E_a may be entirely explained by the measurement uncertainties. Note that the uncertainty on E_a is intrinsic to the measurement method because the wave time arrival determination is sensitive to the rate of variation of signal slope and the low frequency signal used here varies slowly. The use of a higher frequency would have resulted in excessive signal to noise ratio due to attenuation. Despite the uncertainty on E_a, the technique appears to be appropriate for bone

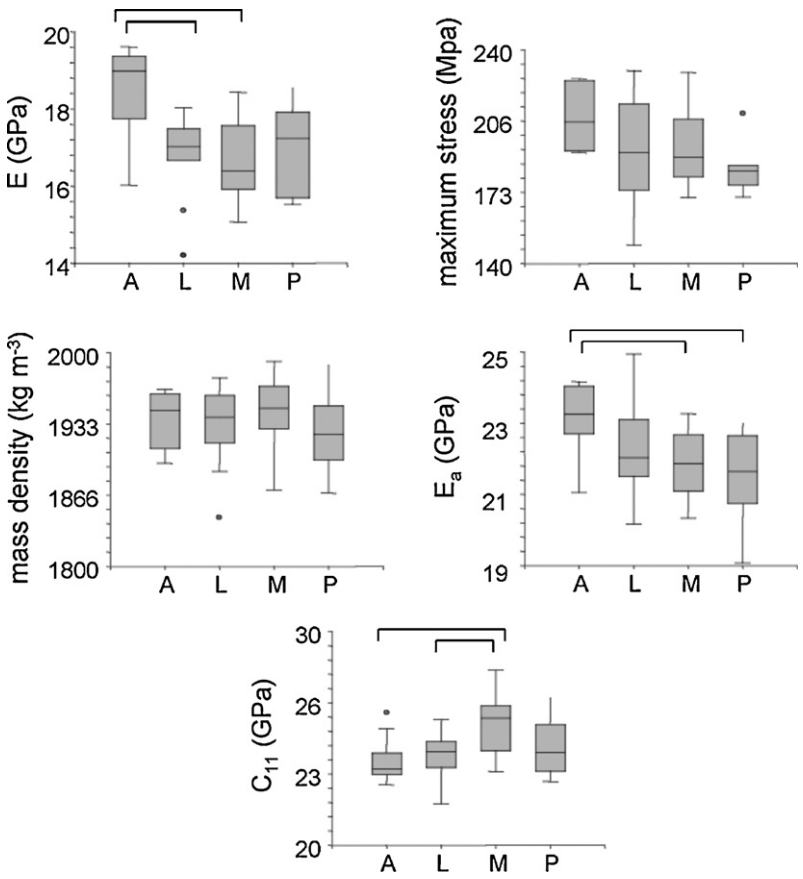

Fig. 8. Box plots of the measured quantities with respect to anatomical quadrants. Box plots give the median value, the interquartile range (IQR: interval between the 25th and 75th percentile, grey area) and the extremum values (T-shaped dark lines). Outliers are indicated with a circle.

characterization because small natural elasticity variations with anatomical position could be probed.

Different authors found low positive [10] or non-significant [11] correlations between elasticity in longitudinal and transverse directions. In the present work a marginal negative correlation was obtained. Interestingly the two-way ANOVA revealed that the negative correlation between E_a and C_{11} is significant ($p = 0.014$) after adjusting for density. We propose two interpretations for these observations: (1) at fixed density, different microscopic organizations at the lamellar levels are possible, resulting in different macroscopic properties. Typically, fiber-reinforced composite samples with a same volume fraction of fibres but differing in average fibres orientations exhibit a negative correlation between elasticity in the longitudinal and transverse directions (the more fibres are in one direction, the less are in the other); (2) the directions of cutting during sample preparation were determined relative to the orientation of the medullar cavity. There is an uncertainty on the alignment of the longitudinal axis of the samples with the local natural frame

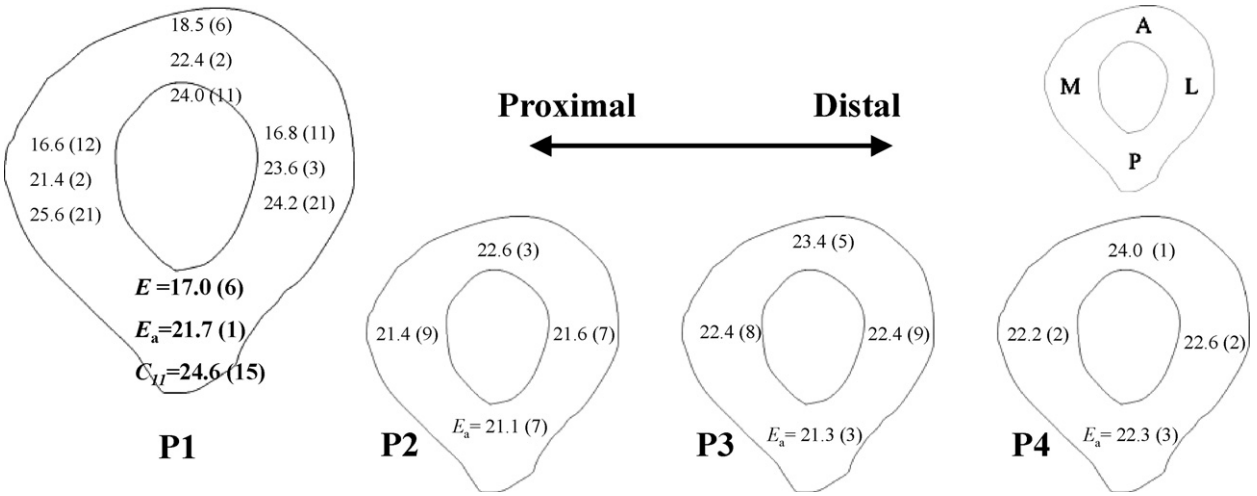

Fig. 9. Variations of measured quantities along the femur length and across quadrants. P1–4 correspond to the four parts of femur cut along the diaphysis (proximal to distal). Only E, C_u and E_a which showed significant variation are represented. For C_u and E which only varied significantly across quadrants, the mean values along the femur length are indicated in P1. Elastic coefficients are in GPa. The number of samples considered in each group for the calculations is given in parenthesis.

of the transversely isotropic bone material. If the material tensor of bone is rotated relative to the measurement frame, the apparent properties in one direction will decrease as the other increase [23]. Finally, note that relatively high correlations between elasticity in the longitudinal and transverse directions of equine bone have also been reported [24]; the latter finding seems related to group of samples with a large variability in elasticity values. It should be noted that precise orientation of the samples in the *transverse plane* was not referenced during sample preparation. However, this is not considered to be a limitation as human bone is approximately isotropic in the transverse plane (see, e.g., experimental results in references [12,21,25] and theoretical considerations for hexagonal symmetry by Yoon and Katz [26]). Furthermore, Espinoza Orías [27] evidenced the transverse isotropic behaviour almost along the entire diaphysis of human femur; they found a moderate orthotropic behaviour close to the femur ends. In particular, samples cut with different orientations in the transverse plane, but at the same anatomical position, are expected to have the same elasticity values.

Note that due to the different types of wave propagation (bar wave and bulk wave) considered (respectively, in longitudinal and transverse directions), two different types of elastic constants (respectively, Young's modulus and stiffness coefficient) were assessed. As a consequence, it is not possible to provide a numerical value for the "usual" anisotropy ratio, i.e., the ratio of two Young's moduli, or alternatively, the ratio of two stiffness coefficients, measured in orthogonal directions.

The main focus of the project was the relationships between anisotropic elasticity and strength σ_{max}. No correlation was found between C_{11} and σ_{max} ($p > 0.2$). Assuming that C_{11} and strength in the transverse direction are related (a relatively strong positive correlation may be expected), our result suggests that strength in the longitudinal and transverse directions may be poorly correlated in some situations. However there is no direct experimental evidence to support this.

Density is most often considered to be the main determinant of bone mechanical properties. Our results indicate low or non-significant correlations of density with elasticity and strength; the higher correlation found was between ρ and σ_{max} ($R = 0.38$; $p < 0.3$). These results may be explained by the fact that compared to many published works the density of the samples investigated was in a narrow range (standard deviation is 30 kg m^{-3}). For instance, Currey [8] observed a strong correlation between bending strength and Young's modulus ($R = 0.94$) using a large data set including bones from 32 animal species that allowed a large range in Young's modulus and density.

Despite the small range of density values, some variations of the mechanical properties were observed. In particular significant variations of elasticity were found between different anatomical quadrants while no significant difference in density could be found (Fig. 8). The significant variations of E_a along the diaphysis reported here may be in contradiction with some published data [3,13,19,21] but is consistent with the report of Bensamoun et al. [28] that bulk wave velocity has significant variations along the diaphysis. These variations may be related to the physiological heterogeneous distribution of *in vivo* strains along the bone diaphysis [29]. The results illustrated in Fig. 8 are consistent with several publications [13,21,27,28] which reported that the elasticity in the longitudinal direction was lower in the posterior quadrant. This result is usually related to the large porosity in the posterior quadrant [30]. The finding that C_{11} is higher in the medial sector has not been reported elsewhere, as far as we know, but is consistent with the trend of the data presented by Espinoza Orías [27].

The results presented in this paper put forward the limitation of using a single quantity, namely density, to account for the mechanical properties of cortical bone in different directions and at various anatomical locations. It is clear from the results that bone samples with similar density may differ significantly in mechanical properties. The fact that femur II and IV had very similar average density (1953 ± 19 and 1958 ± 15 kg m^{-3}, respectively) but significantly differed in average maximum stress (209 ± 16 and 185 ± 20 MPa, respectively), is another manifestation of the aforementioned limitation. The limited practical use of density–mechanical properties relationships possibly arises of the competition between density and microstructural organisation. Generally speaking, the distribution of the mineralised fibers lead to a negative correlation between elasticity in the transverse and longitudinal directions that plays against the amount of matter, which induces a positive correlation (as density increases, elasticity in both direction is expected to increase). In the present investigation where the range of density of the bone samples is narrow it is likely that the microstructural organisation is an important determinant of the measured properties.

5. Conclusion

In the present work, a rich dataset of mechanical properties was obtained with an original multimodal technique that allows for a routine and non-destructive assessment of ultrasonic velocities on plate-like samples with large aspect ratio such as required for three-point bending tests. The technique was originally developed to assess the quality of bone grafts subjected to different sterilization procedures. In this context the method was used routinely to perform in a short time a large number of measurements.

In the present investigation low or non-significant correlations between density and elasticity or strength were found. Elasticity was found to vary with anatomical location while density did not. In addition a small negative correlation was found between elasticity in the longitudinal and transverse directions. These results suggest that isotropic bone tissue models derived from density are unable to account for the variability of elasticity when the density range is narrow (typically ± 30 kg m^{-3}). It was suggested recently that such limitations may be taken into account by modelling the uncertainties on bone properties by using stochastic methods [5,31,32]. Finally, note that our results are not in contradiction with the fact that rather high correlations between density and mechanical properties are obtained in case of large density variability.

The findings of the present work should be balanced by the fact that only four femurs from three donors were used. The conclusions cannot be generalized straightforward to other bones (radius, tibia, etc.) nor to osteoporotic bones.

Acknowledgements

The authors are indebted to Raphaël BARDONNET who was at the origin of the work; to Anne-Isabelle CASSET and Romain IBLED for the preparation of the samples and measurements; to Amena SAÏED for helpful advice on high frequency ultrasonic measurements, and to Pierre GRAVEL for useful advice in signal processing.

Appendix A.

We formulated and tested the hypothesis that the outcome of the correlation between E and E_a was essentially affected by the limited precision of the measurement techniques. Numerical simulations were run on initially perfectly correlated sets of variables ($R^2 = 1$, RMSE = 0), with controlled random errors mimicking the experimental uncertainties. The simulation used a synthetic set of 36 data E_0 generated as $E_0 = 20 + N(0;1.2)$, where $N(a;b)$ is the normal distribution with mean value a and standard deviation b. The values of the standard deviations 1.2 GPa used in the model

correspond to the variability found in the present study for either E or E_a (see Table 1). The mechanical modulus E was modeled as $E^m = E_0 + N(0;0.6)$ and the US modulus E_a as $E_a^m = E_0 + N(0;1.3)$; in these equations we used standard deviations calculated based on the estimated uncertainties for E and E_a. The correlation coefficient was then computed for 10,000 realizations of the synthetic data set. The 95% confidence interval for R was found to be [0.36 0.78]. Since $R = 0.63$ falls within this interval, it was concluded that the measurement uncertainties may explain entirely the lack of correlation between E and E_a.

Conflict of interest statement

There is no conflict of interest.

References

[1] Helgason B, Perilli E, Schileo E, Taddei F, Brynjolfsson S, Viceconti M. Mathematical relationships between bone density and mechanical properties: a literature review. Clin Biomech 2008;23:135–46.
[2] Kaneko TS, Pejcic MR, Tehranzadeh J, Keyak JH. Relationships between material properties and CT scan data of cortical bone with and without metastatic lesions. Med Eng Phys 2003;25:445–54.
[3] Duchemin L, Bousson V, Raossanaly C, Bergot C, Laredo JD, Skalli W, et al. Prediction of mechanical properties of cortical bone by quantitative computed tomography. Med Eng Phys 2007;25:25.
[4] Keyak JH, Rossi SA, Jones KA, Les CM, Skinner HB. Prediction of fracture location in the proximal femur using finite element models. Med Eng Phys 2001;23:657–64.
[5] Laz PJ, Stowe JQ, Baldwin MA, Petrella AJ, Rullkoetter PJ. Incorporating uncertainty in mechanical properties for finite element-based evaluation of bone mechanics. J Biomech 2007;40:2831–6.
[6] Duchemin L, Mitton D, Jolivet E, Bousson V, Laredo J, Skalli W. An anatomical subject-specific FE-model for hip fracture load prediction. Comput Methods Biomech Biomed Eng 2008;30:321–8.
[7] Kober C, Erdmann B, Hellmich C, Sader R, Zeilhofer HF. Consideration of anisotropic elasticity minimizes volumetric rather than shear deformation in human mandible. Comput Methods Biomech Biomed Eng 2006;9:91–101.
[8] Currey JD. What determines the bending strength of compact bone? J Exp Biol 1999;202:2495–503.
[9] Zioupos P. Ageing human bone: factors affecting its biomechanical properties and the role of collagen. J Biomater Appl 2001;15:187–229.
[10] Rho JY, Hobatho MC, Ashman RB. Relations of mechanical properties to density and CT numbers in human bone. Med Eng Phys 1995;17:347–55.
[11] Dong NX, Guo EX. The dependence of transversely isotropic elasticity of human femoral cortical bone on porosity. J Biomech 2004;37:1281–7.
[12] Rho JY. An ultrasonic method for measuring the elastic properties of human tibial cortical and cancellous bone. Ultrasonics 1996;34:777–83.
[13] Ashman RB, Cowin SC, Van Buskirk WC, Rice JC. A continuous wave technique for the measurement of the elastic properties of cortical bone. J Biomech 1984;17:349–61.
[14] Turner CH, Burr DB. In: Cowin SC, editor. Bone mechanics handbook. Boca Raton, FL: CRC Press; 2001.
[15] Achenbach JD. Wave propagation in elastic solids. Amsterdam: North-Holland; 1973.
[16] Ashby MF, Jones DRH. Engineering materials 1. Amsterdam: Elsevier; 2005.
[17] Krautkramer J, Krautkramer H. Ultrasonic testing of materials. Berlin: Springer-Verlag; 1990.
[18] Lide R. Handbook of chemistry and physics. Boca Raton: CRC Press; 1993.
[19] Cuppone M, Seedhom BB, Berry E, Ostell AE. The longitudinal Young's modulus of cortical bone in the midshaft of human femur and its correlation with CT scanning data. Calcif Tissue Int 2004;74:302–9.
[20] Taylor WR, Roland E, Ploeg H, Hertig D, Klabunde R, Warner MD, et al. Determination of orthotropic bone elastic constants using FEA and modal analysis. J Biomech 2002;35:767–73.
[21] Hobatho MC, Rho JY, Ashman RB. In vivo assessment of bone quality by vibration and wave propagation techniques. Part II. Leuven: ACCO Publishing; 1991. pp. 7–32.
[22] Yoon HS, Katz JL. Ultrasonic wave propagation in human cortical bone. II. Measurements of elastic properties and microhardness. J Biomech 1976;9:459–64.
[23] Hoffmeister BK, Smith SR, Handley SM, Rho JY. Anisotropy of Young's modulus of human tibial cortical bone. Med Biol Eng Comput 2000;38:333–8.
[24] Mccarthy RN, Jeffcott LB, Mccartney RN. Ultrasound speed in equine cortical bone: effects of orientation, density, porosity and temperature. J Biomech 1990;23:1139–43.
[25] Katz JL, Yoon HS. The structure and anisotropic mechanical properties of bone. IEEE Trans Biomed Eng 1984;31:878–84.
[26] Yoon HS, Katz JL. Ultrasonic wave propagation in human cortical bone-I. Theoretical considerations for hexagonal symmetry. J Biomech 1976;9:407–12.
[27] Espinoza Orías AA. The relationship between the mechanical anisotropy of human cortical bone tissue and its microstructure. PhD. Thesis, Notre Dame, Indiana; 2005.
[28] Bensamoun S, Ho Ba Tho M-C, Luu S, Gherbezza J-M, De Belleval J-F. Spatial distribution of acoustic and elastic properties of human femoral cortical bone. J Biomech 2004;37:503–10.
[29] Szivek JA, Benjamin JB, Anderson PL. An experimental method for the application of lateral muscle loading and its effect on femoral strain distributions. Med Eng Phys 2000;22:109–16.
[30] Bensamoun S, Gherbezza J-M, De Belleval J-F, Ho Ba Tho M-C. Transmission scanning acoustic imaging of human cortical bone and relation with the microstructure. Clin Biomech 2004;19:639–47.
[31] Nicolella DP, Thacker BH, Katoozian H, Davy DT. The effect of three-dimensional shape optimization on the probabilistic response of a cemented femoral hip prosthesis. J Biomech 2006;39:1265–78.
[32] Macocco K, Grimal Q, Naili S, Soize C. Elastoacoustic model with uncertain mechanical properties for ultrasonic wave velocity prediction; application to cortical bone evaluation. J Acoust Soc Am 2006;119:729–40.